THE POTENTIAL OF SPECTRAL RESAMPLING TECHNIQUES FOR THE SIMULATION OF APEX IMAGERY BASED ON AVIRIS DATA

D. Schläpfer, A. Boerner, and M. Schaepman

Remote Sensing Laboratories (RSL),
Department of Geography, University of Zurich, CH-8057 Zurich, Switzerland
Phone: +41 1 635 52 50, Fax: +41 1 635 68 46, E-mail: dschlapf@geo.unizh.ch

1.   INTRODUCTION

AVIRIS has been widely used for airborne hyperspectral applications but also for inter-calibration experiments with other multispectral and hyperspectral sensors. Special techniques are required for intercalibration and spectral resampling between similarly performing hyperspectral sensors. Some experiments regarding the techniques of spectral simulation for an upcoming hyperspectral instrument are shown herein.

The simulation of a future hyperspectral sensor is essential to obtain an estimate about its performance and to test related algorithms for the expected new data. AVIRIS and other available hyperspectral data shall be used for the simulation of the Airborne PRISM Experiment (APEX) which is initiated by the ESA and will be built in a joint Swiss-Belgian project [Itten et al., 1997]. APEX is an airborne pushbroom imaging spectrometer featuring approximately 300 channels in the wavelength range between 400 and 2500 nm. One of the major technological achievements is the increased spectral resolution of 5 nm for APEX compared to 10 nm of AVIRIS between 400 and 1100 nm wavelength. Another goal is the use of 'pushbroom' technology at a high number of up to 1000 pixels per line in order to simulate spaceborne instruments.

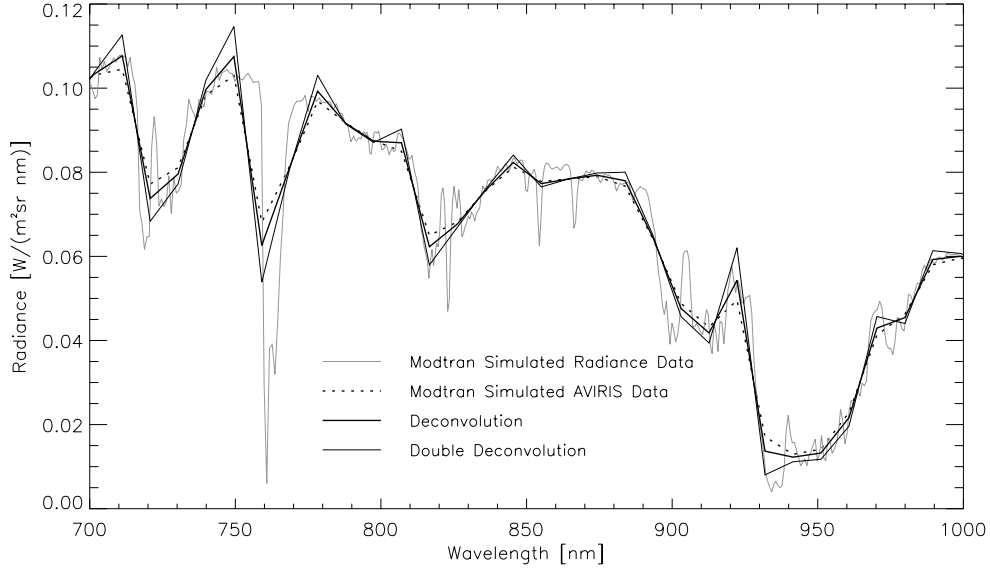Three major approaches are suggested to simulate APEX data:

- A ray tracer model simulates the optical path from the ground through the instrument optics to the sensors to characterize the influence of the single instrument parts on the data quality.
- The realistic radiometric and geometric performance analysis is based on currently available hyperspectral instruments such as AVIRIS.
- A third approach is the demonstration of the technology using a hyperspectral pushbroom instrument.

Only the second approach is described in this paper. The goal is the construction of data cubes of the same spectral and spatial resolution as the final APEX data products, but with the radiometric performance and the internal geometry of current AVIRIS data. The pushbroom instrument simulation had to be dropped due to the lack of an appropriately performing sensor.

The spatial resampling has been widely studied in the past and can therefore be treated with standard algorithms. Bilinear interpolation can be used for raw data resampling [Kellenberger, 1996; Schowengerdt, 1997] while geocoding procedures can be used for the resampling to a fixed spatial resolution in a georeferenced product [Schläpfer et al, 1998]. Thus, this paper concentrates on problems related to spectral resampling.

2.   SPECTRAL DECONVOLUTION

Deconvolution is usually used for the signal recovery of filtered continuos signals. Deconvolution methods used for spectral reconstruction are different. The raw hyperspectral signal has not been affected by a continuous filter - moreover it has been weighted by the channel dependent spectral response functions. The individual channels of AVIRIS (and other imaging spectrometers) are overlapping each other in order to achieve a continuous coverage of the spectrum. This fact is a condition for the application of a deconvolution technique. The overlapping area of the response functions (see Figure 2) can be corrected by subtracting the weighted neighboring channel value from the original signal:

Figure 1: **The effect of deconvolution on MODTRAN-simulated AVIRIS data (at 30% reflectance). The absorption features are emphasized depending on the radiance in the adjacent bands.**

$$L_{i,dec} \;=\; (L_i - L_{i+1}w_i - L_{i-1}w_{i-1})\frac{R_i}{R_i - w_i - w_{i-1}}\,, \tag{1}$$

The single weighting factors are given as follows:

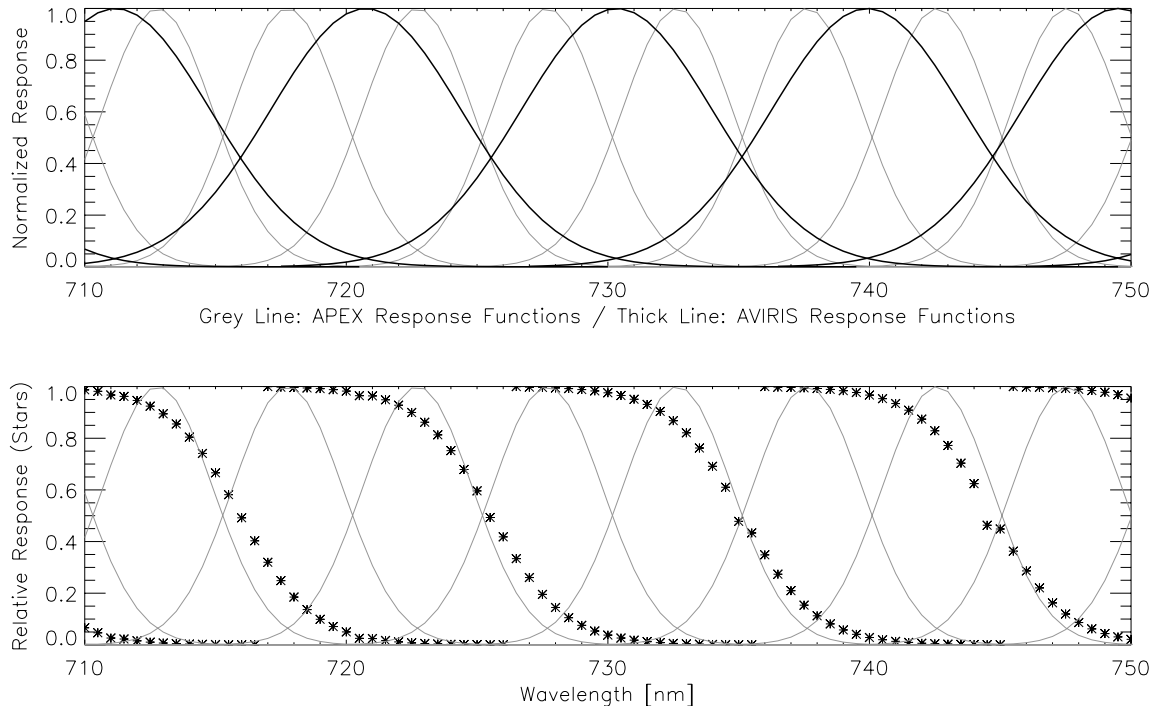The integral response of channel i: $\qquad R_i \;=\; \int r_i(\lambda)d\lambda$,

and the overlap weighting factor between channel i and channel i+1: $w_i \;=\; 0.5\int min[\dot r(\lambda)_i,\, r(\lambda)_{i+1}]d\lambda$.

The response functions r_i for each channel is a result from the laboratory calibration. It is usually assumed to be Gaussian for high resolution imaging spectrometers. Thus, it has to be calculated from center wavelength and 'Full Width at Half Maximum' (FWHM) for each channel at a high spectral resolution (e.g. 0.5 nm). The factor of 0.5 for the neighbor-weighting factors was chosen to account for the simultaneous registration by two channels in this 'overlapping' wavelength range. Moreover, it helps to avoid erroneous over-deconvolution which introduces a significant amount of noise. The full deconvolution using a factor of 1.0 is referred as 'double deconvolution' in the sections below.

As the integrated response R_i is usually normalized it has not to be calculated for all channels. Notice that this normalization can not be used anymore if the energy efficiency of the channels differs from one to another. In that case all response functions of a sensor focal plane should be normalized according to their relative efficiency.

The spectral deconvolution (as discussed in Eq. (1)) increases the signature of sharp spectral absorption features by decreasing the effective bandwidth of each channel artificially. It does not gain information about absorption features originally not present in the data and about the real position of these features. This technique shall therefore be used prior to spectral resampling algorithms in order to avoid information loss, but it does certainly not increase the information content of a hyperspectral image.

The use of Fourier transformation for this kind of deconvolution proved to be inadequate and therefore less accurate than this directly integrating approach. Fourier deconvolution handles spectrally continuously moving filters perfectly while the changing response functions at discrete wavelengths of the imaging spectrometer channels have to be treated separately [Madisetti and William, 1998; Richards, 1993].

Figure 2: Spectral response functions of AVIRIS and APEX for a few spectral channels (top) and the normalized resampling function (Stars; bottom) for the mixing of AVIRIS data to a continuous spectrum.

3. HIGH RESOLUTION SPECTRUM RECONSTRUCTION

After the channels are deconvolved they are recombined to a highly resolved spectrum. This combination is done using a sum-to-one approach. The individual overlapping channels are combined to a higher resolved spectrum at a factor of 20 and more compared to the original sensor spectral resolution. The response functions of all overlapping channels at a specific wavelength are summed and normalized to a total value of 1 such that

$$\overline{r_i(\lambda)} = \frac{r_i(\lambda)}{\sum_n r_n(\lambda)}, \ \forall(i \in n).$$

(2)

The number of simultaneous channels n for AVIRIS was limited to 3 in this test, but could also be increased for greater overlaps between non-adjacent channels. The derivation of this 'mixing function' from AVIRIS response is shown in Figure 2 (bottom) for a few channels.

The radiance is then reconstructed using the relative response information from Eq. (2) and the deconvolved radiance information from Eq. (1) at the given high internal spectral resolution:

$$L(\lambda) = \sum_i L_i \overline{r_i(\lambda)}.$$

(3)

This mixed radiance retrieved from original data can then be used for the simulation of any sensor of similar characteristics as the original sensor. The deconvolution helps to prevent from losing sharp spectral features – a spectral smoothing effect occurs in the simulated data if no deconvolution is applied.

4. ADJUSTMENT TO ATMOSPHERIC ABSORPTION FEATURES

The highly resolved radiance data has finally to be convolved to the response functions of the simulated sensor. The spectral resolution of the APEX is planned to be approximately twice as high as the AVIRIS characteristics in the visible/near infrared range of the spectrum (400 to 1100 nm). Sharp spectral features of the atmosphere (as well as of ground targets) can therefore not be simulated accurately using the deconvolution-recombination technique ('DRT') described above.

We introduced MODTRAN [Berk et al., 1989; Kneisys et al., 1995] simulations of the radiance for both sensors to take these artefacts into account. First, the radiance at the sensor is simulated for the AVIRIS data at average atmospheric conditions and ground reflectance (here $\rho = 0.2$). The output of the radiative transfer code is then spectrally resampled using the technique given above. The relation of this result $L_{M, sim, j}$ to the original directly MODTRAN-simulated APEX data $L_{M, j}$ is taken as correction factor to the convolution of the reconstructed radiance of the new response functions. The radiance simulation for a new channel j is then described as:
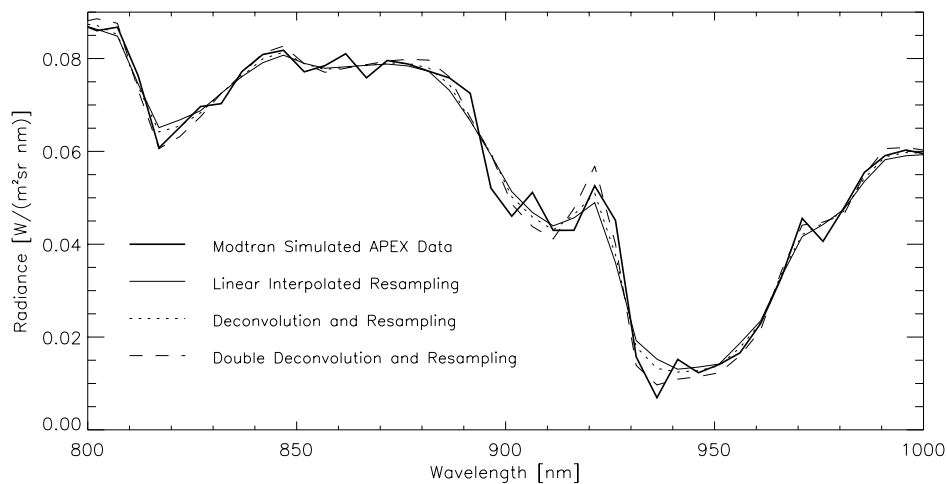
$$L_j = \frac{L_{M, j}}{L_{M, sim, j}} \cdot \frac{\int L(\lambda) r_j(\lambda) d\lambda}{\int r_j(\lambda) d\lambda}, \qquad (4)$$

where $r_j(\lambda)$ is the spectral response function of the new APEX channel.
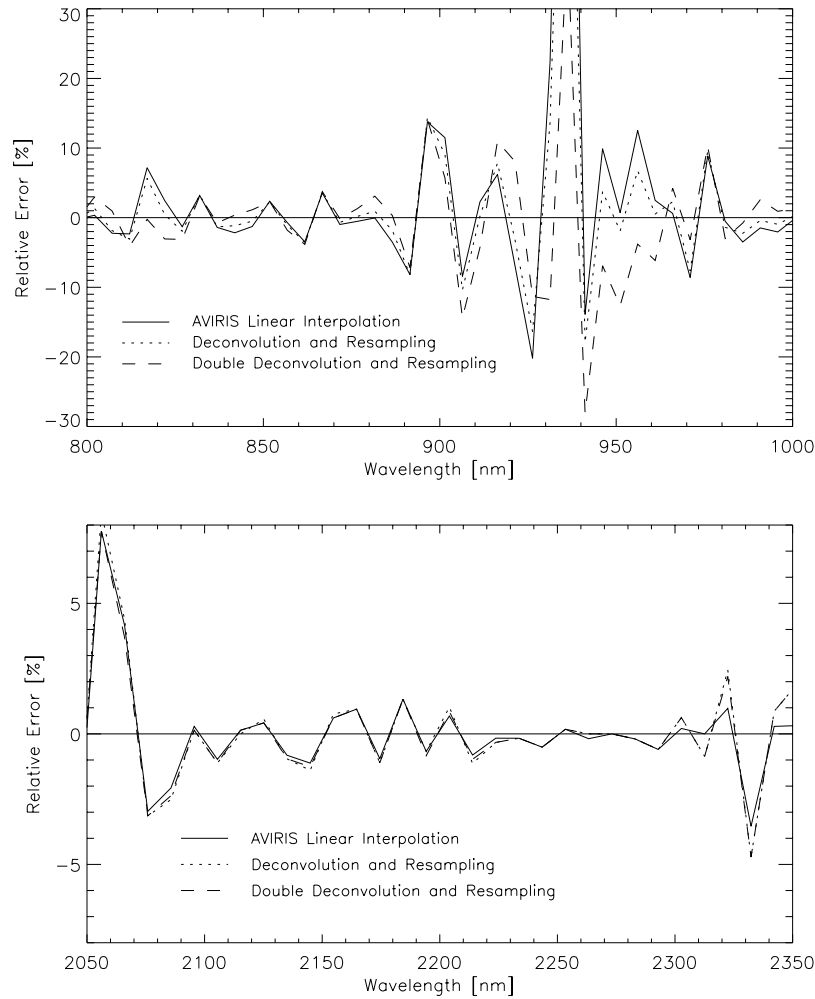
More accurate atmospheric feature reconstruction is required for the simulation at varying flight altitude and viewing geometry. For such a full radiometric simulation, the following atmospheric processing steps are proposed:

1) Correction of the original AVIRIS image to ground reflectance, using an atmospheric correction procedure (e.g. ATCOR [Richter et al., 1997]),
2) spatial resampling of the image during a geocoding process (e. g. PARGE [Schläpfer et al., 1998]) or by bilinear interpolation to the required pixel dimensions,
3) spectral resampling of the ground reflectance spectra using the 'DRT'- technique given by equations (1) to (3),
4) modelling the at-sensor-radiance using a radiative transfer calculation (inverse atmospheric correction) or a sensor simulation program.

Using this procedure, the ground reflectance values are resampled instead of the at-sensor radiances. The equations (1) to (3) therefore have to be adopted for the resampling of spectral reflectance (ρ) instead of L. Such a procedure is a consistent radiometric approach while resampling on reflectance data. It simulates the atmospheric features accurately. However, additional sharp ground reflectance features such as in geology and limnology can not be reconstructed although the resolution is seemingly increased.

Figure 3:   **Resampling of MODTRAN-simulated AVIRIS data to APEX resolution within a water vapor absorption region using deconvolution techniques.**
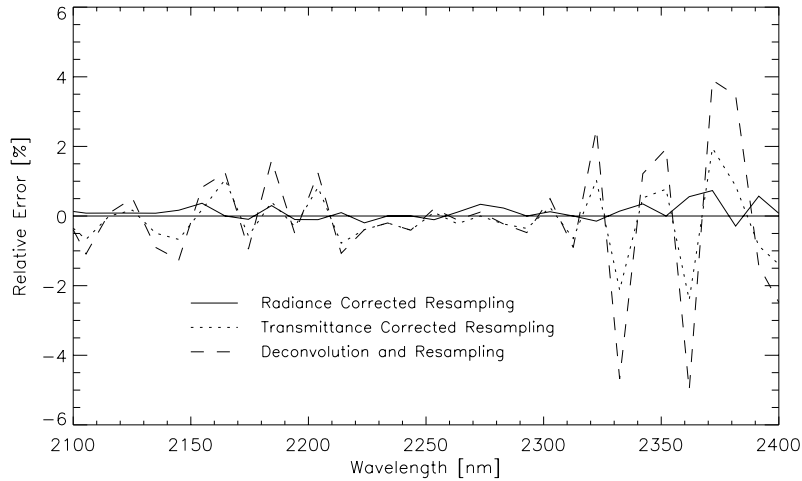
Figure 4: Relative difference of various resampling options to APEX spectral resolution for two wavelength ranges. TOP: Differences related to atmospheric absorption features and the resampling from 10 nm to 5 nm spectral resolution. BOTTOM: Resampling effect at same resolution (10 nm) of the instruments but at different central wavelength position.

5.   RESULTS AND ERROR ANALYSES

The evaluation of the different techniques is performed based on MODTRAN simulated radiance spectra at varying (linear) background reflectance. This approach was chosen since no simultaneous AVIRIS and APEX data are currently available for direct evaluation purposes.

The difference between APEX spectra taken directly from MODTRAN simulation to three different simulation options was first evaluated. An example is depicted in Figure 3. If the double deconvolution is applied, the features are pronounced to unrealistic values, while the normal deconvolution (using the weighting factor 0.5) increases the accuracy of the resampled spectrum in comparison to the expected APEX raw spectrum. The non-deconvolved linear interpolation of AVIRIS data to APEX resolution shows the highest differences especially in sharp features.

The error analysis (see Figure 4) shows large differences up to 15% for all three methods in the wavelength regions where APEX is defined with 5 nm resolution bands. The spectral resampling itself is not able to

Figure 5: Relative errors of atmospheric corrected resampling methods in comparison to pure deconvolution resampling technique.

reconstruct sharp spectral features from the 'low' resolution AVIRIS data (10 nm). However, the errors are significantly lower, if deconvolved AVIRIS data is used instead of linearly interpolated data (see also Table 1).

The influence of deconvolution is not significant at wavelength ranges where APEX and AVIRIS spectral resolution is approximately the same (i.e. above 1100 nm wavelength). The deconvolution even increases the deviations at wavelengths where only little signal is available. It thus may amplify noisy artefacts instead of the real spectral features.

The differences decrease if atmospheric features are introduced during the processing (see Figure 5). If only the transmittance influence is corrected, the improvement is not significant, but with a radiance based radiometric correction much better results are achieved than by deconvolution only.

Table 1 lists the RMS and averaged errors for five simulation techniques evaluated over all 300 simulated APEX channels. Full double deconvolution clearly increases the errors in comparison to linear interpolation, while normal deconvolution decreases the errors significantly. The radiance based atmospheric adjustment decreases the error by another significant factor. It has yet to be shown, how a full atmospheric correction technique will influence this result.

Table 1: Average Error estimates for various spectral resampling techniques (averaged over all available APEX channels at varying MODTRAN background reflectance).

Method	Relative Error (RMS)	Average Relative Error
Linear Interpolation	1.3 - 2.7%	5.7 - 7.5%
Deconvolution resampling	1.1 - 1.6%	5.9 - 6.7%
Double Deconvolution	> 10%	> 13%
Transmittance Correction	1.1 - 1.3%	5.7 - 6.1%
Radiance Correction	0.9 - 1.0%	2.2 - 2.9%

6.   CONCLUSIONS

A technique was described and tested which allows spectral resampling of existing hyperspectral data (AVIRIS) to the characteristics of upcoming and planned sensors (e.g. APEX). The technique will be used to produce an APEX data cube from AVIRIS data for the evaluation of the APEX processing chain. The data will help to evaluate atmospheric and geometric correction algorithms as well as to gain experiences with radiometric consistent future APEX data.

The data loss of the technique is minimal due to the combination of spectral deconvolution and spectrum reconstruction. However, a noticeable amount of noise may be added to the spectra by the deconvolution, which decreases the accuracy in simulated narrow and low reflective bands.

The importance of atmospheric correction for sensor simulation from existing image data has been emphasized. It has been shown that the spectral resampling has to be done in the reflectance domain as soon as the conditions of the simulated image are not the same as in the original image.

Standard correction algorithms combined with the depicted deconvolution-resampling technique will be applied to available hyperspectral imagery to simulate reflectance APEX cubes. Such retrieved reflectance images will be introduced into a ray tracing sensor simulation model which is currently being developed at RSL to simulate APEX image cubes under various atmospheric and geometric conditions.

7.   REFERENCES

Berk A., Bernsten L.S., and Robertson D.C., 1989: *MODTRAN: A Moderate Resolution Model for LOWTRAN7.* Air Force Geophysics Laboratory, GL-TR-89-0122, Hanscom AFB, MA, 38 pp.

Itten K.I., Schaepman M., De Vos L., Hermans L., Schlaepfer H., and Droz F., 1997: APEX-Airborne Prism Experiment a New Concept for an Airborne Imaging Spectrometer. *Proceedings of the Third International Airborne Remote Sensing Conference and Exhibition*, Vol. I, ERIM International Inc., Copenhagen (DK), pp. 181-188

Kellenberger, T., 1996: *Erfassung der Waldfläche in der Schweiz mit multispektralen Satellitenbiddaten, Grundlagen, Methodenentwicklung und Anwendung*; Dissertation, Remote Sensing Series Vol. 28, Geographisches Institut der Universität Zürich, pp. 90

Kneisys F.X., Abreu L.W., Anderson G.P., Chetwynd J.H., Shettle E.P., Berk A., and et al., 1995: *The MODTRAN 2/3 and LOWTRAN Model.* Abreu L.W. and Anderson G.P. (ed.), Appendix C, Ontar Corporation, North Andover, MA, 267 pp.

Madisetti V.K., and William B.D., 1998: *The Digital Signal Processing Handbook.* CRC Press LLC, Boca Raton, FL(USA), Sections III and IV

Richards J.A., 1993: *Remote Sensing Digital Image Analysis*, 2nd Edition. Springer Verlag, Berlin, 340 pp.

Richter R., 1997: Correction of atmospheric and topographic effects for high-spatial-resolution satellite imagery. *SPIE Vol. 3071, Alg. for Mult. and Hyp. Im. III*, Orlando, pp. 216-224

Schläpfer D., Schaepman M., and Itten K.I., 1998: PARGE: Parametric Geocoding Based on GCP-Calibrated Auxiliary Data. Descour and Shen (Eds.), *SPIE Vol. 3438, Imaging Spectrometry IV*, San Diego, pp. 334-344

Schowengerdt R.A., 1997: *Remote Sensing: Models and Methods for Image Processing. 2nd Ed.*, Academic Press, pp. 522